# Structural Optimization of the Links of a Parallel Spherical Manipulator

TR–CIM–01–05 May, 2001

**Florence Bidault**

Departement of Industrial and Mechanical Engineering
Ecole Centrale de Nantes, France

**Jorge Angeles, and Chin-Pun Teng**

Centre for Intelligent Machines, McGill University,
Montreal, Quebec, H3A 2K6, Canada

Centre for Intelligent Machines (CIM) and
Department of Mechanical Engineering
McGill University, Montreal, Quebec, Canada

# Abstract

We propose a structural optimization approach to the design of the links of a parallel spherical manipulator, the *Agile Wrist*, to minimize its weight, for a given nominal load condition. A static analysis of the *Agile Wrist* is first conducted. This analysis allowed us to model the loads that were introduced for the finite element analysis and for the optimization procedure on the Pro/Mechanica Structure module.

# Résumé

Ce rapport traite d'une approche pour l'optimisation structurelle des maillons d'un manipulateur parallèle sphérique, le *Poignet Agile*, afin de minimiser le poids total du manipulateur pour une charge donnée correspondant à la charge supportée par le *Poignet Agile* dans sa position nominale. Nous présentons tout d'abord l'analyse statique du *Poignet Agile*, qui fut ensuite introduite pour l'analyse par éléments finis et la procédure d'optimisation réalisées toutes les deux sous le module Structure Pro/Mechanica dans le logiciel Pro/Engineer.

# Contents

# List of Figures

# Chapter 1

# Introduction

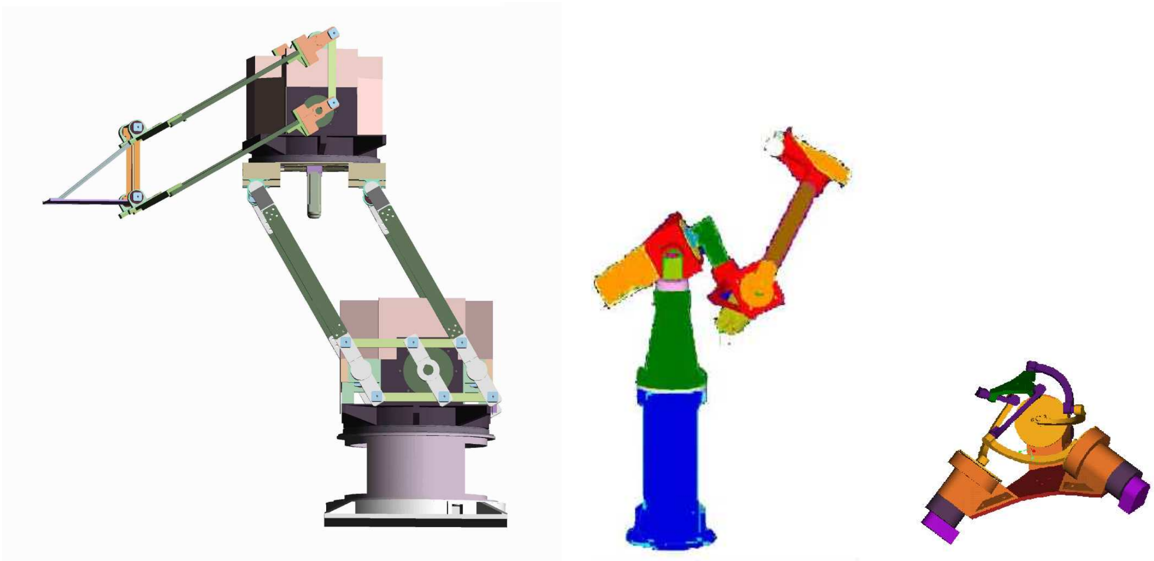

(a) (b) (c)

Figure 1.1: The 11-DOF robot: (a) the SCARA-motion generator; (b) the Cuatro arm; (c) the Agile Wrist

The *Agile Wrist* (AW) is a spherical manipulator designed as a module of an 11-degree-of-freedom (dof) long-reach robot. This robot is in fact designed as a cascade of three modules (See Fig. 1):

- (a) The gross manipulator, realizing four-dof positioning tasks of the SCARA type;
- (b) The intermediate module, the *Cuatro Arm*, a four-dof architecture responsible for the positioning of a point of its terminal link;
- (c) The *Agile Wrist*, a three-dof parallel spherical wrist whose base is rigidly attached to the end link of the *Cuatro Arm* and whose moving plate carries the tool.

Accuracy and precision in the execution of the task of the wrist are essential since the robot is intended to operate on fragile objects such as the fuselage of aircraft: any errors in the positioning of the tool could lead to expensive damage. This is why a parallel spherical wrist with an isotropic configuration was chosen for the orientation of the tool. Parallel manipulators have the advantage of supporting heavier loads than their serial counterparts, since each parallel chain takes a part of the load, besides providing a better accuracy and a higher velocity. Parallel spherical wrists are used to orient an object in space. Different architectures have already been proposed and studied (Asada and Cro Granito 1985; Gosselin and Angeles 1989; Craver 1989). We adopted the *isotropic* architecture proposed by Gosselin and Hamel (1994), because kinetostatic isotropy ensures a uniform velocity control and a better orientational accuracy in a region centred around the isotropic posture.

A factor that can significantly reduce the accuracy of the end-effector is the flexibility of the manipulator links due to external payloads and inertial loading. For the most part, the geometric shape and the cross-section dimensions of the links of manipulators are designed quite arbitrarily, with simple shapes and constant cross sections. Current structural optimization technology and the use of highly accurate CNC machine tools enable the designers to produce optimum, if more complex, shapes; an efficient selection of the design parameters could improve the overall stiffness of a link without making it heavier. A general trend in the design of lighter and stiffer structures has led to the use of sophisticated materials, like graphite fibre-reinforced composites with the consequent slandering of structural components. These components should ensure that no failure can occur under a given range of loads, which has motivated intensive research in the area of structural optimization, a very active field since Schmidt (1960) set forth an approach for coupling finite element analysis and nonlinear programming. The research work reported here lies in the realm of structural optimization: it deals with the optimum design of the links of the *Agile Wrist* in order to enhance the load-carrying capacity of the *Cuatro Arm*, while minimizing its weight. We focus here on the shaping of the links, rather than on material selection.

For optimization purposes, we start with a static analysis, whereby all links are assumed rigid, in order to estimate the constraint wrenches acting at the revolute joints. When performing a force analysis on a link, we consider two kinds of forces: (a) those exerted by the environment, coming from the weight of the tool and the loads acting on the latter, and (b) the constraint forces that are transmitted through the joints connecting a link to the its neighbours. Once the wrenches exerted on each link are determined, we undertake an optimization procedure by means of Finite Element Analysis (FEA), which we do here with the aid of the Pro/Mechanica Structure module of Pro/Engineer. As an objective function to minimize, we selected the weight of the links, subject to bounds on the stresses in order to ensure the highest stiffness.

# Chapter 2

# Background

## 2.1 Description of the Wrist Architecture

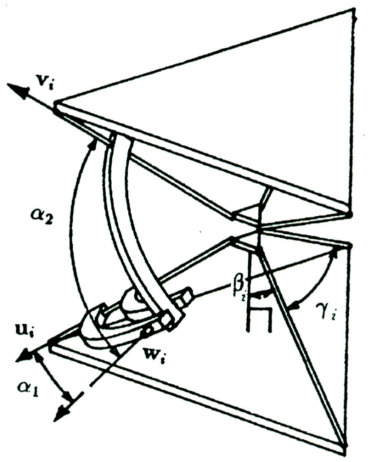


Figure 2.1: Geometric parameters of Craver's shoulder module

The wrist architecture consists of two main elements, the base, which is rigidly attached to the end-link of the *Cuatro Arm*, and the moving platform, which is free to undergo arbitrary rotations with respect to the centre of the wrist. The *Agile Wrist* is a particular case of the shoulder module described by Craver (1989) and sketched in Fig. 2.1. This general architecture could be thought of as composed of two pyramidal modules, the base and the moving platform, that have as a common apex the centre of the wrist. The two plates are coupled by means of three identical legs, each of these composed of two links coupled to each other by means of a revolute joint. The link coupled to the base is called the *proximal link* and that coupled to the moving platform is called the *distal link*. Both links are coupled to the platforms via revolute joints, so that the whole mechanism comprises nine revolute joints. The geometric parametrization used to describe the foregoing architecture is often the one depicted in Fig. 2.1. The unit vectors directed along the revolute axes of the actuators at the base are referred to as vectors $\mathbf{u}_i$, $i = 1, 2, 3$, the ones along the revolute axes at the moving platform are referred to as vectors $\mathbf{v}_i$, $i = 1, 2, 3$ and the unit vectors directed along the axes of the intermediate

joints are noted $\mathbf{w}_i$, $i = 1, 2, 3$. The angles between neighbouring joint axes, $\alpha_1$ and $\alpha_2$, define a specific architecture.
The direct kinematics of spherical wrists was solved by Gosselin et al. (1992), while Gosselin and Hamel (1994) conducted an architecture optimization based on the global conditioning index (Gosselin and Angeles, 1991) and showed that a wrist with angles $\alpha_1$ and $\alpha_2$ equal to 90° has the best overall index. They then chose this architecture for a camera-orienting device called the *Agile Eye*. Moreover, Gosselin and his team reported a closed-form solution for the

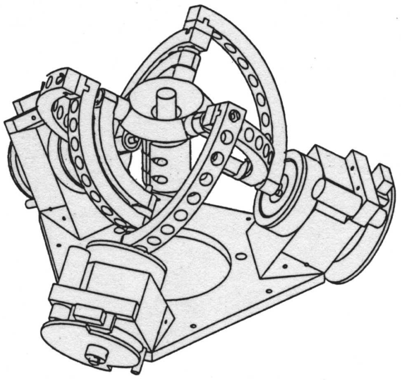

Figure 2.2: the Agile Eye

direct kinematics problem (Gosselin and Gagné 1995) as well as the dynamics model of this manipulator for this architecture (Gosselin and Gagné 1995). The design of the *Agile Wrist* is based on that of the *Agile Eye* (Fig. 2.2), mainly because of its isotropic architecture, but redesign work was deemed necessary. As a matter of fact, the *Agile Wrist* is to be attached to a moving arm; thus, one of the objectives while designing the *Agile Wrist* was to make it as light as possible. Moreover, due to the shape and the weight of the tool which will be installed on top of the upper platform, the design and dimensioning of the wrist was revised. A simulation showed that some collisions between the tool and the moving links occured, thus reducing dramatically the workspace of the wrist. That is why an alternative design for the proximal link was proposed. Instead of using tree parts, two arcs and a fastener for the proximal link, a single curved link was devised. The original and the new alternative designs are displayed in Fig. 2.1.

## 2.2 Isotropy

This concept was first introduced in robot design by Salisbury and Craig (1982) while using the *condition number* of the Jacobian matrix to quantify the accuracy of the linear transformation between joint rates and Cartesian velocities. The condition number of a matrix $\mathbf{A}$ is defined as (Golub and Von Loan 1983):

$$k(\mathbf{A}) = ||\mathbf{A}||\ ||\mathbf{A}^{-1}|| \tag{2.1}$$

where $||\mathbf{A}||$ is any matrix norm; in particular, we can use the *Frobenius norm* $||.||_F$, defined as:

$$||\mathbf{A}||_F = \sqrt{\frac{1}{n}\mathrm{tr}(\mathbf{A}\mathbf{A}^T)} \tag{2.2}$$

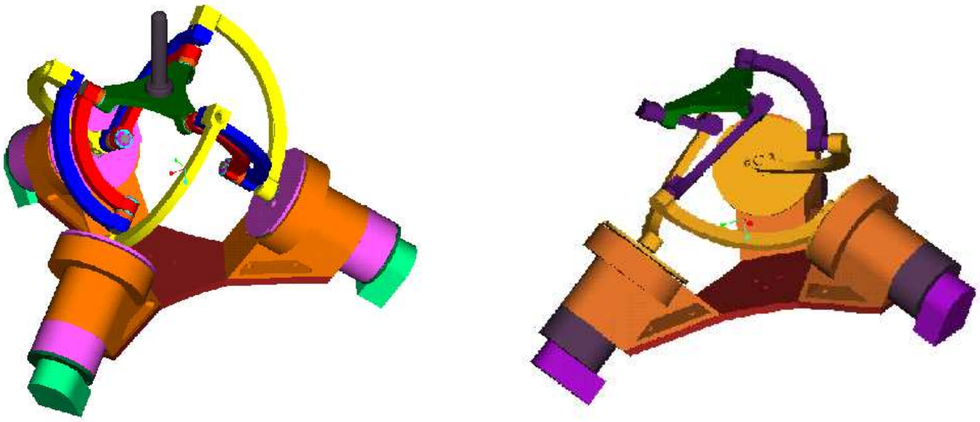

(a) AW with Gosselin's design (b) AW with the alternative design

Figure 2.3: The original and the new design of the Agile Wrist

for an $n \times n$ matrix $\mathbf{A}$. Another possible matrix norm is the 2-norm, defined as:

$$||\mathbf{J}||_2 = \max_{\mathbf{x} \neq 0} \left\{ \frac{||\mathbf{A}\mathbf{x}||}{||\mathbf{x}||} \right\} \tag{2.3}$$

where the vector-norm in the curly brackets is the Euclidean norm. The condition number $\kappa(\mathbf{A})$ under the 2-norm turns out to be the ratio of the largest singular value $\sigma_l$ of $\mathbf{A}$ to the smallest one $\sigma_s$ (Golub and Von Loan 1989):

$$\kappa(\mathbf{A}) = \frac{\sigma_l}{\sigma_s} \tag{2.4}$$

Note that $\kappa(\mathbf{A})$ tends to infinity in the presence of a singular $\mathbf{A}$: When $\mathbf{A}$ is the Jacobian $\mathbf{J}$ of a manipulator, the manipulator gains or loses one or more degrees of freedom. When $\kappa(\mathbf{A})$ equals unity, an isotropic configuration occurs: a unit joint-rate vector, or a unit joint-torque vector, produces a constant-norm angular-velocity vector of the end-effector (EE) or, correspondingly, balances a constant-norm moment applied at the EE, for arbitrary values of the components of the vector of joint rates or of joint torques (Gosselin and Lavoie 1993). Thus, $\kappa(\mathbf{A})$ can also be used to measure the orientation-error amplification for one given robot posture (Angeles 1997). To evaluate the overall kinematic performance on the whole workspace, a *global kinematic index* can be used (Gosselin and Hamel 1994).

# Chapter 3

# Kinetostatic Analysis

While the kinematic analysis of parallel spherical wrists has been the subject of many publications, the static and force analysis has received less attention. Yi, Freeman and Tesar (1992) proposed a force and stiffness transmission analysis for a spherical shoulder mechanism by means of the Jacobian matrix. This kind of analysis provides the designer with useful information to select the appropriate actuators, but in the case of spherical wrists, only moments are taken into account by the analysis, the forces at the joints remaining indeterminate. While designing the links of the *Agile Wrist*, we had to ensure that they can withstand the load acting on the tool, but no moments are created if this load is a force acting on a line passing through the centre of the wrist, which is the case when the *Agile Wrist* is in its nominal, isotropic posture.

Another approach consists in considering a force transmission index, often called stiffness (Gosselin 1990), which is in fact, rather a sensitivity index (Angeles, Bulca, Arenson, Angeles, and Slutski, 1998; Ranjbaran, Angeles and Kecskeméthy, 1997) that reflects the influence that a "small" change in the required task produces on the posture of the manipulator. While optimizing the architecture to obtain an isotropic configuration, this index (Gosselin and Angeles 1989; 1991) was in fact already taken into account; this is why we did not pursue this approach.

In our case, the base of the *Agile Wrist* can be oriented so that it is then possible to determine the moment exerted by the weight of the tool at the centre of the wrist by using a "Jacobian" approach and then evaluating the loading moment acting on the most heavily loaded leg. The ensuing kinetostatic analysis enables us to determine wh!ich maximum moment amplitude the *Agile Wrist* can withstand with the prescribed actuators.

## 3.1 Kinematics of the Agile Wrist and of the $i^{th}$ Leg

In order to evaluate the loading moment acting on a leg, we first compute the moments acting on the end effector of the *Agile Wrist*. We then determine the torque at each actuated joint. To determine the moments taken by one leg, we use the Jacobian matrix of the serial chain formed by a leg. As a matter of fact, each leg of the *Agile Wrist* is a serial RRR spherical wrist (Fig. 3.1): the first joint couples the base with the proximal link, the second one couples the proximal link with the distal link and the last one couples the distal link with the end effector. This serial wrist is orthogonal, i.e., its neighbouring revolute axes are laid out at 90°.

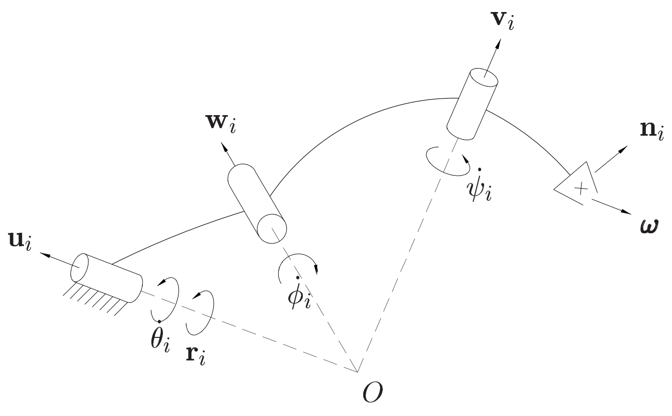


Figure 3.1: THE $i_{th}$ LEG OF THE AW

The angular velocity $\boldsymbol{\omega}$ of the end effector of the *Agile Wrist* can be expressed in terms of the joint rates of the $i^{th}$ leg:

$$\dot{\theta}_i \mathbf{u}_i + \dot{\phi}_i \mathbf{w}_i + \dot{\psi}_i \mathbf{v}_i = \boldsymbol{\omega} \tag{3.1}$$

To eliminate the unactuated rates of the previous expression, eq.(3.1) is dot-multiplied by the cross-product $\mathbf{w}_i \times \mathbf{v}_i$, thereby obtaining:

$$\dot{\theta}_i(\mathbf{w}_i \times \mathbf{v}_i).\ \mathbf{u}_i = (\mathbf{w}_i \times \mathbf{v}_i).\ \boldsymbol{\omega} \tag{3.2}$$

Upon assembling the scalar equations (3.2) for $i = 1, 2, 3$, the desired kinematic equations are obtained, namely:

$$\mathbf{B}\dot{\boldsymbol{\theta}} + \mathbf{A}\boldsymbol{\omega} = \mathbf{0}, \qquad \dot{\boldsymbol{\theta}} = \begin{bmatrix} \dot{\theta}_1 \\ \dot{\theta}_2 \\ \dot{\theta}_3 \end{bmatrix} \tag{3.3}$$

where $\dot{\boldsymbol{\theta}}$ is the vector of actuated joint rates at the base of the *Agile Wrist*, and matrices $\mathbf{A}$ and $\mathbf{B}$ are (Gosselin and Angeles 1990):

$$\mathbf{A} = \begin{bmatrix} (\mathbf{v}_1 \times \mathbf{w}_1)^T \\ (\mathbf{v}_2 \times \mathbf{w}_2)^T \\ (\mathbf{v}_3 \times \mathbf{w}_3)^T \end{bmatrix} \tag{3.4}$$

$$\mathbf{B} = \mathrm{diag}[\mathbf{u}_1 \times \mathbf{w}_1.\mathbf{v}_1,\ \mathbf{u}_2 \times \mathbf{w}_2.\mathbf{v}_2,\ \mathbf{u}_3 \times \mathbf{w}_3.\mathbf{v}_3] \tag{3.5}$$

If $\mathbf{B}$ is nonsingular, then:

$$\dot{\boldsymbol{\theta}} = -\mathbf{B}^{-1}\mathbf{A}\boldsymbol{\omega} \tag{3.6}$$

Now, for the static analysis, let $\mathbf{n}$ be the moment acting on the end effector, taken at the centre of the wrist.

The power developed by the load and the motors, $\Pi_e$ and $\Pi_m$, respectively, are given as:

$$\Pi_e = \mathbf{n}^T \boldsymbol{\omega}, \qquad \Pi_m = \boldsymbol{\tau}^T \dot{\boldsymbol{\theta}} \tag{3.7}$$

The Principle of Virtual Work, under kinetostatic, conservative conditions, then leads to:

$$\mathbf{n}^T \boldsymbol{\omega} = \boldsymbol{\tau}^T \dot{\boldsymbol{\theta}} \tag{3.8}$$

Equations (3.6) and (3.8) lead, in turn, to:

$$\mathbf{n}^T \boldsymbol{\omega} = -\boldsymbol{\tau}^T \mathbf{B}^{-1} \mathbf{A} \boldsymbol{\omega}, \qquad \forall \ \boldsymbol{\omega} \tag{3.9}$$

Equation (3.9) holding for any velocity vector $\boldsymbol{\omega}$ of the end effector, the above equation leads to:

$$\mathbf{n}^T = -\boldsymbol{\tau}^T \mathbf{B}^{-1} \mathbf{A} \ \text{ or } \ \mathbf{n} = -\mathbf{A}^T \mathbf{B}^{-T} \boldsymbol{\tau} \tag{3.10}$$

Equation (3.10) enables us to determine the moment acting on the wrist for a given torque vector, the torques being provided by the motors. By inverting this equation, we can obtain the vector $\boldsymbol{\tau}$ of actuator torques, for a given moment acting on the wrist, i.e.,

$$\boldsymbol{\tau} = -\mathbf{B}\mathbf{A}^{-1}\mathbf{n} = \begin{bmatrix} \tau_1 \\ \tau_2 \\ \tau_3 \end{bmatrix} \tag{3.11}$$

The moment $\mathbf{n}$ is in fact distributed among all three legs, with the $i^{th}$ leg taking up a part $\mathbf{n}_i$ of $\mathbf{n}$, so that:

$$\mathbf{n} = \mathbf{n}_1 + \mathbf{n}_2 + \mathbf{n}_3 \tag{3.12}$$

To find $\mathbf{n}_i$, let $\boldsymbol{\mu}_i$ (see in Fig. 3.1) be the three-dimensional joint-torque vector of the $i^{th}$ leg and $\mathbf{n}_i$ defined as above. That is,

$$\boldsymbol{\mu}_i = \begin{bmatrix} \tau_i \\ 0 \\ 0 \end{bmatrix}, \qquad i = 1, 2, 3 \tag{3.13}$$

which is known from eq.(3.11).

The static relation between $\boldsymbol{\mu}_i$ and $\mathbf{n}_i$ is similar to that of any serial manipulator, i.e.:

$$\mathbf{J}_i^T \mathbf{n}_i = \boldsymbol{\mu}_i \tag{3.14}$$

where

$$\mathbf{J}_i = [\mathbf{u}_i \ \mathbf{w}_i \ \mathbf{v}_i] \tag{3.15}$$

By inverting eq.(3.14), we obtain:

$$\mathbf{n}_i = \mathbf{J}_i^{-T} \boldsymbol{\mu}_i \tag{3.16}$$

which is the share of the load taken up by the $i^{th}$ leg. To calculate $\mathbf{J}_i^{-1}$, reciprocal bases (Brand 1965) can be used, thus obtaining

$$\Delta_i = \det(\mathbf{J}_i) = \mathbf{u}_i \times \mathbf{w}_i.\mathbf{v}_i \tag{3.17}$$

$$\mathbf{J}_i^{-1} = \frac{1}{\Delta_i} \begin{bmatrix} (\mathbf{w}_i \times \mathbf{v}_i)^T \\ (\mathbf{v}_i \times \mathbf{u}_i)^T \\ (\mathbf{u}_i \times \mathbf{w}_i)^T \end{bmatrix} \tag{3.18}$$

whence,

$$\mathbf{n}_i = \mathbf{J}_i^{-1} \boldsymbol{\mu}_i = \frac{\mathbf{w}_i \times \mathbf{v}_i}{\mathbf{u}_i \times \mathbf{w}_i.\mathbf{v}_i} \tau_i \tag{3.19}$$

The load $\mathbf{n}_i$ taken by the $i^{th}$ leg is normal to the plane defined by the second and third-revolute axes of the $i^{th}$ leg. This could not be otherwise, for each of these revolutes being unactuated, it can exert a moment on the links that it couples only in a direction lying in a plane normal to its axis. Moreover, the moment exerted by the end effector onto the distal link must be equal and of opposite sign to that exerted by the proximal link onto the same distal link, under static conditions

## 3.2 Load Moment Acting on the Most Heavily Loaded Leg

An important loading condition for the *Agile Wrist* occurs when the base of the *Agile Wrist* is oriented vertically and the *Agile Wrist* is in its nominal isotropic posture, as depicted in Fig. 3.2, in which $\mathbf{i}$ is a unit vector in the downward vertical direction. The most heavily loaded leg appears here to be the second leg.

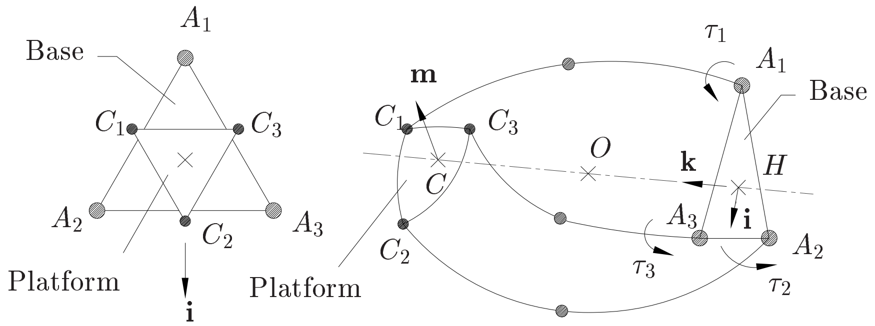


Figure 3.2: POSTURE OF THE AW FOR THE KINETOSTATIC ANALYSIS

To perform the kinetostatic analysis, we assume that the weight of the tool and of the moving platform is concentrated at the centre of the moving platform, point $C$ in Fig. 3.2. The centre of this platform is, in fact, point $O$, while $R_m$ is the distance $OC_i$, where $C_i$ is the centre of the revolute joint coupling the $i^{th}$ leg with the moving platform. The force vector at point $C$ is noted $\mathbf{f} = F\mathbf{i}$ and the vector pointing from $O$ to $C$ is noted $\mathbf{c} = R_m\mathbf{k}$; vector $\mathbf{i}$, directed along the vertical, lies in a plane parallel to the base, and vector $\mathbf{k}$, directed along the horizontal, is collinear with a line passing through $H$, the centre of the base, and $O$, the centre of the wrist.

The unit vectors $\mathbf{u}_i$, $i = 1, 2, 3$, form an orthonormal frame which will be used as a co-ordinate frame. The nominal configuration for the distal vectors is characterized by:

$$\mathbf{v}_{10} = -\mathbf{u}_3, \qquad \mathbf{v}_{20} = -\mathbf{u}_1, \qquad \mathbf{v}_{30} = -\mathbf{u}_2 \tag{3.20}$$

and for the intermediate unit vectors by:

$$\mathbf{w}_{10} = \mathbf{u}_2, \qquad \mathbf{w}_{20} = \mathbf{u}_3, \qquad \mathbf{w}_{30} = \mathbf{u}_1 \tag{3.21}$$

In the frame $\mathcal{U}(O,\ \mathbf{u}_1,\ \mathbf{u}_2,\ \mathbf{u}_3)$, the coordinates of the points $A_1$ and $H$ are $(d\ ,\ 0\ ,\ 0)$ and $(d/3\ ,\ d/3\ ,\ d/3)$, respectively. Since vector $\mathbf{k}$ has the same direction as the vector pointing from $H$ to $O$, and vector $\mathbf{i}$ the same one as the vector pointing from $A_1$ to $H$, vectors $\mathbf{k}$ and $\mathbf{i}$ are readily obtained after a normalization process. Vector $\mathbf{j}$ can then be obtained by means of the cross-product: $\mathbf{j} = \mathbf{k} \times \mathbf{i}$.

$$\mathbf{k} = -\frac{\sqrt{3}}{3}\mathbf{u}_1 - \frac{\sqrt{3}}{3}\mathbf{u}_2 - \frac{\sqrt{3}}{3}\mathbf{u}_3 \tag{3.22}$$

$$\mathbf{i} = -\frac{\sqrt{6}}{3}\mathbf{u}_1 + \frac{\sqrt{6}}{6}\mathbf{u}_2 + \frac{\sqrt{6}}{6}\mathbf{u}_3 \tag{3.23}$$

The moment $\mathbf{n}_O$ with respect to the centre of the wrist is given by:

$$\mathbf{n}_O = \mathbf{c} \times \mathbf{f} + \mathbf{n}_C \tag{3.24}$$

where $\mathbf{n}_C$ is the load moment vector with respect to point $C$, here considered as equal to zero. From equation (3.24) we obtain:

$$\mathbf{n}_O = R_m F(\mathbf{i} \times \mathbf{k}) \tag{3.25}$$

We determine the torque at each actuated joint with relation (3.11). For the nominal configuration, $-\mathbf{BA}^{-1}$ reduces to the $3 \times 3$ identity matrix, eq.(3.11) and (3.19) thus leading to:

$$\boldsymbol{\tau}_0 = \mathbf{n}_0 \tag{3.26}$$

and

$$\mathbf{n}_{i_0} = \tau_{i0}\mathbf{u}_i \tag{3.27}$$

where $\tau_{i0}$ is given by:

$$\tau_{i0} = R_m F(\mathbf{i} \times \mathbf{k}).\mathbf{u}_i = \frac{\sqrt{2}}{2} R_m F \tag{3.28}$$

The moment at the distal joint coupling the distal link with the moving platform is, then,

$$\mathbf{n}_{i_0} = \frac{\sqrt{2}}{2} R_m F \mathbf{u}_i \tag{3.29}$$

## 3.3 Evaluation of the Load-Carrying Capacity

According to Servo Systems Inc., of Montville, NJ, the manufacturer of the *Agile Wrist* direct-drive motors, these can provide a peak torque equal to 0.353 Nm. Relation (3.10) enables us to determine the moments that the *Agile Wrist* can balance for eight different cases:

$$\tau_1 = \pm 0.353 \text{ Nm},\ \tau_2 = \pm 0.353 \text{ Nm and } \tau_3 = \pm 0.353 \text{ Nm}$$

For the nominal configuration, eq.(3.10) yields the moment:

$$\mathbf{n}_O = \tau_1 \mathbf{u}_1 + \tau_2 \mathbf{u}_2 + \tau_3 \mathbf{u}_3 \tag{3.30}$$

The components of the moment $\mathbf{n}_O$ in frame $\mathcal{V}(O, \mathbf{i}, \mathbf{j}, \mathbf{k})$ are:

$$M_x = \frac{\sqrt{3}}{3}(\tau_1 - \tau_2 - \tau_3) \tag{3.31}$$

$$M_y = \frac{\sqrt{2}}{2}(\tau_2 - \tau_3) \tag{3.32}$$

$$M_z = \frac{\sqrt{6}}{6}(-2\tau_1 + \tau_2 + \tau_3) \tag{3.33}$$

If we assume that the moments about the centre of the wrist are due only to the weight of the tool, which acts at the centroid of the moving platform, that is, $|M_y| = R_m F$, then the mass of the tool that this manipulator can support is about 0.7 kg—$R_m$ is about 74 mm, the radius of the distal link. However, this estimate is done for the worst loading condition, i.e., with the base oriented vertically.

The numerical results are displayed in Table 3.1

| $\tau_1$ (Nm) | $\tau_2$ (Nm) | $\tau_3$ (Nm) | $M_x$ (Nm) | $M_y$ (Nm) | $M_z$ (Nm) |
|---|---|---|---|---|---|
| 0.353 | 0.353 | 0.353 | −0.204 | 0 | 0 |
| −0.353 | 0.353 | 0.353 | −0.611 | 0 | 0.576 |
| −0.353 | −0.353 | 0.353 | −0.204 | −0.499 | 0.288 |
| −0.353 | 0.353 | −0.353 | −0.204 | −0.499 | 0.288 |
| −0.353 | −0.353 | −0.353 | 0.204 | 0 | 0 |
| 0.353 | −0.353 | 0.353 | 0.204 | −0.499 | −0.288 |
| 0.353 | −0.353 | −0.353 | 0.611 | 0 | −0.576 |
| 0.353 | 0.353 | −0.353 | 0.204 | 0.499 | −0.288 |

Table 3.1: Numerical values of the moments about the centre of the wrist provided by the actuators upon reaching their peak torque

# Chapter 4

# Static Analysis of the Agile Wrist

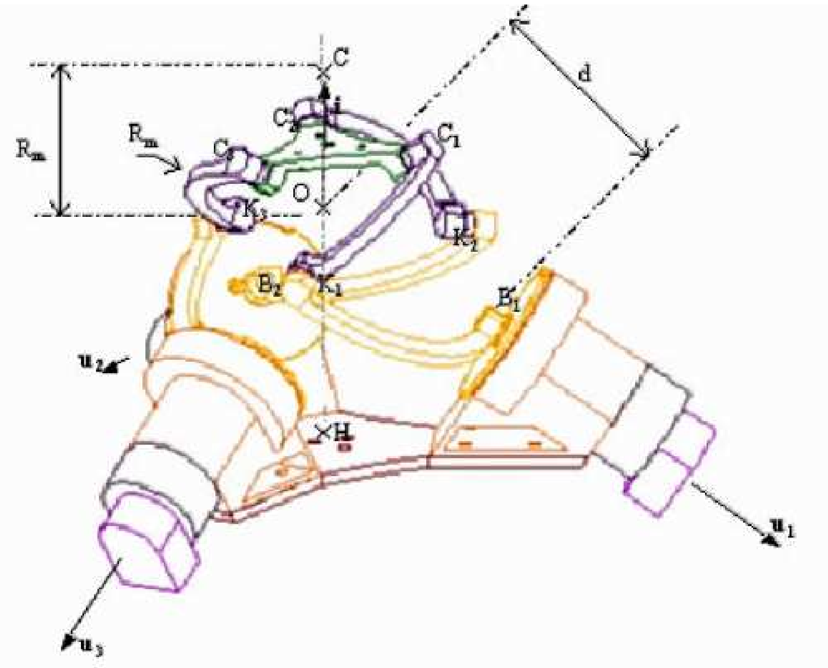


Figure 4.1: Layout of the Agile Wrist

In the sections below we determine the loads acting on the *Agile Wrist* links when the centroids of the two platforms are on the same vertical line and a vertical load due to the total weight of the tool and the moving platform is exerted at the centroid of the moving platform, point $C$ on Fig. 4.1. To find the forces and moments acting on the links, we use free-body diagrams (FBD) for each moving link, i.e., the moving platform, the distal and the proximal links.

## 4.1 General Analysis

With the base fixed, the *Agile Wrist* is composed of seven moving links: the moving platform, three distal links and three proximal links. These links are coupled by revolute joints. We thus have nine revolute joints in the whole mechanism and $9 \times 5 = 45$ unknown reaction components. Indeed, by virtue of the nature of revolute joints, the moment about any point along each 'unactuated joint axis is zero. By the same token, the moment about an actuated revolute is known. Upon applying the static equilibrium conditions, we obtain $7 \times 6 = 42$ equations, the problem thus being statically indeterminate. To solve it, we need additional information or engineering hypotheses. In fact, we decided to solve the forgoing indeterminacy by replacing the unactuated revolute joints by cylindrical joints. The moment component about any point along each cylindrical joint is equal to that of the corresponding revolute but now the force along the axis of the cylindrical joint is zero. The number of unknowns is then reduced to $3 \times 5 + 6 \times 4 = 42$, and the system becomes determinate. Such an approach was also adopted by Larochelle and McCarthy (1992) while discussing the static analysis of spherical $nR$ kinematic chains with joint friction. Even if they did not pretend to replace the revolute joints by cylindrical joints, they stated that due to the geometry of the joints, no force is transmitted along the axis of unactuated joints. It is noteworthy that the forgoing joint replacement does not have any effect on the kinematics of the *Agile Wrist*; moreover, if implemented in the design, this replacement avoids overconstraints and eases the assembly of the mechanism.

## 4.2 Statics of the Moving Platform

### 4.2.1 Forces and Moments Acting on the Moving Platform

If we isolate the moving platform and consider the external forces and moments on that moving link, we find two kinds of forces: the weight of the tool and the moving platform and the forces coming from the kinematic constraints at the joints coupling the moving platform with the distal link. The notation below is used:

- $\mathbf{f}$ is the external force due to the weight of the moving platform and the tool, which acts at the centroid $C$ of the moving platform;
- $\mathbf{f}_{dm_i}$ is the force exerted by the $i^{th}$ distal link ($i = 1, 2, 3$) on the moving platform, and acting at point $C_i$, that we consider at the middle of the cylindrical joint;
- $\mathbf{m}_{dm_i}$ is the moment at point $C_i$, exerted by the $i^{th}$ distal link ($i = 1, 2, 3$) on the moving platform.

Due to the nature of the cylindrical joints, the moment and force components along the axis of the cylindrical joint coupling the $i^{th}$ distal link with the moving platform vanish. The wrenches $\mathbf{w}_{dm_i} = [\mathbf{m}_{dm_i}{}^T \quad \mathbf{f}_{dm_i}{}^T]^T$ exerted by the $i^{th}$ distal link ($i = 1, 2, 3$) on the moving platform, expressed in frame $\mathcal{U} = (O\ ,\ \mathbf{u}_1\ ,\ \mathbf{u}_2\ ,\ \mathbf{u}_3)$, then take the form:

$$\mathbf{w}_{dm_1} = \begin{bmatrix} U_{dm_1} \\ V_{dm_1} \\ 0 \\ X_{dm_1} \\ Y_{dm_1} \\ 0 \end{bmatrix} \qquad \mathbf{w}_{dm_2} = \begin{bmatrix} 0 \\ V_{dm_2} \\ W_{dm_2} \\ 0 \\ Y_{dm_2} \\ Z_{dm_2} \end{bmatrix} \qquad \mathbf{w}_{dm_3} = \begin{bmatrix} U_{dm_3} \\ 0 \\ W_{dm_3} \\ X_{dm_3} \\ 0 \\ Z_{dm_3} \end{bmatrix}$$

### 4.2.2 Equilibrium Equations

By applying the equilibrium condition for forces and moments, projected on the different axes of frame $\mathcal{U}$, we obtain six equations. Those for forces are:

$$\mathbf{f} + \sum_{i=1}^{3} \mathbf{f}_{dm_i} = \mathbf{0} \tag{4.1}$$

or, in component form:

$$\begin{aligned} \tfrac{\sqrt{3}}{3}||\mathbf{f}|| + X_{dm_1} + X_{dm_3} &= 0 \\ \tfrac{\sqrt{3}}{3}||\mathbf{f}|| + Y_{dm_1} + Y_{dm_2} &= 0 \\ \tfrac{\sqrt{3}}{3}||\mathbf{f}|| + Z_{dm_2} + Z_{dm_3} &= 0 \end{aligned}$$

The vector equation of moment equilibrium is obtained below by taking moments about $C$, which is the centroid of the moving platform (Fig. 4.1), i.e.,

$$\sum_{i=1}^{3} (\mathbf{m}_{dm_i} + (\mathbf{n}_{C_i} - \mathbf{n}_C) \times \mathbf{f}_{dm_i}) = \mathbf{0} \tag{4.2}$$

or, in component form:

$$\begin{aligned} R_m(Y_{dm_1} - Z_{dm_3}) + U_{dm_1} + U_{dm_3} &= 0 \\ R_m(Z_{dm_2} - X_{dm_1}) + V_{dm_1} + V_{dm_2} &= 0 \\ R_m(X_{dm_3} - Y_{dm_2}) + W_{dm_2} + W_{dm_3} &= 0 \end{aligned}$$

## 4.3 Statics of the Distal Links

### 4.3.1 Forces and Moments Acting on the $i^{th}$ Distal Link

When isolating the $i^{th}$ distal link, we only consider force constraints transmitted through the cylindrical joints coupling this link with the moving platform and with the corresponding proximal link. The weight of the link is neglected. Likewise,

- $\mathbf{f}_{md_i}$ is the force exerted by the moving platform on the $i^{th}$ distal link ($i = 1, 2, 3$), which acts at point $C_i$;
- $\mathbf{m}_{md_i}$ is the moment about point $C_i$, exerted by the moving platform on the $i^{th}$ distal link ($i = 1, 2, 3$);
- $\mathbf{f}_{pd_i}$ is the force exerted by the $i^{th}$ proximal link on the $i^{th}$ distal link ($i = 1, 2, 3$) and acting at point $K_i$, the centre of the intermediate cylindrical joint coupling the two links;
- $\mathbf{m}_{pd_i}$ is the moment about point $K_i$, exerted by the $i^{th}$ proximal link on the $i^{th}$ distal link ($i = 1, 2, 3$).

The corresponding wrenches are:

$$\mathbf{w}_{md_1} = \begin{bmatrix} U_{md_1} \\ V_{md_1} \\ 0 \\ X_{md_1} \\ Y_{md_1} \\ 0 \end{bmatrix} \qquad \mathbf{w}_{md_2} = \begin{bmatrix} 0 \\ V_{md_2} \\ W_{md_2} \\ 0 \\ Y_{md_2} \\ Z_{md_2} \end{bmatrix} \qquad \mathbf{w}_{md_3} = \begin{bmatrix} U_{md_3} \\ 0 \\ W_{md_3} \\ X_{md_3} \\ 0 \\ Z_{md_3} \end{bmatrix}$$

where, apparently, $\mathbf{w}_{md_i} = -\mathbf{w}_{dm_i}$.

The wrenches, in frame $\mathcal{U}$, are:

$$\mathbf{w}_{pd_1} = \begin{bmatrix} U_{pd_1} \\ 0 \\ W_{pd_1} \\ X_{pd_1} \\ 0 \\ Z_{pd_1} \end{bmatrix} \qquad \mathbf{w}_{pd_2} = \begin{bmatrix} U_{pd_2} \\ V_{pd_2} \\ 0 \\ X_{pd_2} \\ Y_{pd_2} \\ 0 \end{bmatrix} \qquad \mathbf{w}_{pd_3} = \begin{bmatrix} 0 \\ V_{pd_3} \\ W_{pd_3} \\ 0 \\ Y_{pd_3} \\ Z_{pd_3} \end{bmatrix}$$

### 4.3.2 Equilibrium Equations

By applying the force equilibrium condition, we obtain

$$\mathbf{f}_{pd_i} + \mathbf{f}_{md_i} = \mathbf{0}, \quad i = 1,\ 2,\ 3 \tag{4.3}$$

Thus, we can readily solve for the new force components (three new unknowns per leg, and three equilibrium equations per leg). In component form

$$\begin{array}{lll} X_{pd_1} + X_{md_1} = 0 & X_{pd_2} = 0 & X_{md_3} = 0 \\ Y_{md_1} = 0 & Y_{pd_2} + Y_{md_2} = 0 & Y_{pd_3} = 0 \\ Z_{pd_1} = 0 & Z_{md_2} = 0 & Z_{pd_3} + Z_{md_3} = 0 \end{array}$$

Through the moment equilibrium condition projected on the different axes of frame $\mathcal{U}$, we obtain, for each leg, three vector equations and, consequently, for all the legs, nine scalar equations. The static equilibrium condition, for each leg, with moments about point $K_i$, are given by:

$$\mathbf{m}_{pd_i} + \mathbf{m}_{md_i} + (\mathbf{n}_{C_i} - \mathbf{n}_{K_i}) \times \mathbf{f}_{md_i} = \mathbf{0}, \quad i = 1,\ 2,\ 3 \tag{4.4}$$

We then obtain nine scalar equations, namely,

$$\begin{array}{ccc} U_{pd_1} + U_{md_1} = 0 & U_{pd_2} + Y_{pd_2} R_m = 0 & U_{md_3} - Z_{md_3} R_m = 0 \\ V_{md_1} - X_{md_1} R_m = 0 & V_{pd_2} + V_{md_2} = 0 & V_{pd_3} + Z_{md_3} R_m = 0 \\ W_{pd_1} + X_{md_1} R_m = 0 & W_{md_2} - Y_{pd_2} R_m = 0 & W_{pd_3} + W_{md_3} = 0 \end{array}$$

## 4.4 Statics of the Proximal Links

### 4.4.1 Forces and Moments Acting on the $i^{th}$ Proximal Links

We also neglect the weight of the proximal link when considering the forces exerted on it. Here,

- $\mathbf{f}_{dp_i}$ is the force exerted by the $i^{th}$ distal link on the $i^{th}$ proximal link $(i = 1, 2, 3)$ , which acts at point $K_i$;
- $\mathbf{m}_{md_i}$ is the moment about $C_i$ exerted by the moving platform on the $i^{th}$ distal link $(i = 1, 2, 3)$;
- $\mathbf{f}_{bd_i}$ is the force exerted by the base on the $i^{th}$ proximal link $(i = 1, 2, 3)$ and acting at point $B_i$, the centre of the revolute joint coupling the $i^{th}$ proximal link with the base;

- $\mathbf{m}_{pd_i}$ is the moment about $B_i$, exerted by the base on the $i^{th}$ proximal link ($i = 1, 2, 3$).

The associated wrenches, in frame $\mathcal{U}$, are

$$\mathbf{w}_{dp_1} = \begin{bmatrix} U_{dp_1} \\ 0 \\ W_{dp_1} \\ X_{dp_1} \\ 0 \\ Z_{dp_1} \end{bmatrix} \qquad \mathbf{w}_{dp_2} = \begin{bmatrix} U_{dp_2} \\ V_{dp_2} \\ 0 \\ X_{dp_2} \\ Y_{dp_2} \\ 0 \end{bmatrix} \qquad \mathbf{w}_{dp_3} = \begin{bmatrix} 0 \\ V_{dp_3} \\ W_{dp_3} \\ 0 \\ Y_{dp_3} \\ Z_{dp_3} \end{bmatrix}$$

$$\mathbf{w}_{bp_1} = \begin{bmatrix} 0 \\ V_{bp_1} \\ W_{bp_1} \\ X_{bp_1} \\ Y_{bp_1} \\ Z_{bp_1} \end{bmatrix} \qquad \mathbf{w}_{bp_2} = \begin{bmatrix} 0 \\ V_{bp_2} \\ W_{bp_2} \\ X_{bp_2} \\ Y_{bp_2} \\ Z_{bp_2} \end{bmatrix} \qquad \mathbf{w}_{bp_3} = \begin{bmatrix} 0 \\ V_{bp_3} \\ W_{bp_3} \\ X_{bp_3} \\ Y_{bp_3} \\ Z_{bp_3} \end{bmatrix}$$

### 4.4.2 Equilibrium Equations

By applying the force equilibrium conditions, we obtain:

$$\mathbf{f}_{dp_i} + \mathbf{f}_{bp_i} = \mathbf{0}, \quad i = 1,\ 2,\ 3 \tag{4.5}$$

and thus, we can readily solve for the new unknown reactions. In component form, we have:

$$\begin{array}{lll} X_{dp_1} + X_{bp_1} = 0 & X_{bp_2} = 0 & X_{dp_3} + X_{bp_3} = 0 \\ Y_{dp_1} + Y_{dp_1} = 0 & Y_{dp_2} + Y_{bp_2} = 0 & Y_{bp_3} = 0 \\ Z_{bp_1} = 0 & Z_{dp_2} + Z_{bp_2} = 0 & Z_{dp_3} + Z_{bp_3} = 0 \end{array}$$

By means of the moment equilibrium condition projected onto the axes of frame $\mathcal{U}$, we obtain, for each leg, three equations and, consequently, for all the legs, nine equations. The vector equilibrium equations, for each leg, with moments about the point $B_i$, are given by:

$$\mathbf{m}_{dp_i} + \mathbf{m}_{bp_i} + (\mathbf{n}_{K_i} - \mathbf{n}_{A_i}) \times \mathbf{f}_{dp_i} = \mathbf{0}, \quad i = 1,\ 2,\ 3 \tag{4.6}$$

We then obtain the corresponding nine scalar equations, i.e.,

$$\begin{array}{lll} U_{dp_1} + U_{bp_1} = 0 & U_{bp_2} = 0 & U_{bp_3} = 0 \\ V_{bp_1} = 0 & V_{dp_2} + V_{bp_2} = 0 & V_{bp_3} = 0 \\ W_{bp_1} = 0 & W_{bp_2} = 0 & W_{dp_3} + W_{bp_3} = 0 \end{array}$$

### 4.4.3 Summary

The components of the wrenches due to the effect of the external forces and moments acting on each link are given below, as expressed in frame $\mathcal{U}$.

Wrenches acting at the distal links:

$$\mathbf{w}_{md_1} = \frac{\sqrt{3}}{3}\begin{bmatrix} 0 \\ FR_m \\ 0 \\ F \\ 0 \\ 0 \end{bmatrix} \qquad \mathbf{w}_{pd_1} = \frac{\sqrt{3}}{3}\begin{bmatrix} 0 \\ 0 \\ -FR_m \\ -F \\ 0 \\ 0 \end{bmatrix} \tag{4.7}$$

$$\mathbf{w}_{md_2} = \frac{\sqrt{3}}{3}\begin{bmatrix} 0 \\ 0 \\ FR_m \\ 0 \\ F \\ 0 \end{bmatrix} \qquad \mathbf{w}_{pd_2} = \frac{\sqrt{3}}{3}\begin{bmatrix} -FR_m \\ 0 \\ 0 \\ 0 \\ -F \\ 0 \end{bmatrix} \tag{4.8}$$

$$\mathbf{w}_{md_3} = \frac{\sqrt{3}}{3}\begin{bmatrix} FR_m \\ 0 \\ 0 \\ 0 \\ 0 \\ F \end{bmatrix} \qquad \mathbf{w}_{pd_3} = \frac{\sqrt{3}}{3}\begin{bmatrix} 0 \\ -FR_m \\ 0 \\ 0 \\ 0 \\ -F \end{bmatrix} \tag{4.9}$$

Wrenches acting at the proximal links:

$$\mathbf{w}_{dp_1} = \frac{\sqrt{3}}{3}\begin{bmatrix} 0 \\ 0 \\ FR_m \\ F \\ 0 \\ 0 \end{bmatrix} \qquad \mathbf{w}_{bp_1} = \frac{\sqrt{3}}{3}\begin{bmatrix} 0 \\ 0 \\ 0 \\ -F \\ 0 \\ 0 \end{bmatrix} \tag{4.10}$$

$$\mathbf{w}_{dp_2} = \frac{\sqrt{3}}{3}\begin{bmatrix} FR_m \\ 0 \\ 0 \\ 0 \\ F \\ 0 \end{bmatrix} \qquad \mathbf{w}_{bp_2} = \frac{\sqrt{3}}{3}\begin{bmatrix} 0 \\ 0 \\ 0 \\ 0 \\ -F \\ 0 \end{bmatrix} \tag{4.11}$$

$$\mathbf{w}_{dp_3} = \frac{\sqrt{3}}{3}\begin{bmatrix} 0 \\ FR_m \\ 0 \\ 0 \\ 0 \\ F \end{bmatrix} \qquad \mathbf{w}_{bp_3} = \frac{\sqrt{3}}{3}\begin{bmatrix} 0 \\ 0 \\ 0 \\ 0 \\ 0 \\ -F \end{bmatrix} \tag{4.12}$$

### 4.4.4 Numerical Results

Since we assumed that the wrenches are applied at the centre of the revolute and cylindrical joints, we determine their effect at the centre of the surface of each end of the link by taking into account the geometry of the link. Forces are unchanged and moments are given by the relation:

$$\mathbf{m}_B = \mathbf{m}_A + (\mathbf{n}_B - \mathbf{n}_A) \times \mathbf{f}_A \tag{4.13}$$

A safety factor of 1.5 that corresponds to a service factor for supporting light machinery, shaft or motor driven, according to the AISC code (Shigley 1989), was taken into account; the loads below, expressed in frame $\mathcal{U}$, were introduced at the surfaces of the distal and proximal links, respectively.

- Distal link:

$$\mathbf{w}_{md_1} = \begin{bmatrix} 0 \\ 2.7063 \\ 0.2165 \\ 43.3013 \\ 0 \\ 0 \end{bmatrix} \qquad \mathbf{w}_{pd_1} = \begin{bmatrix} 0 \\ 0.3031 \\ -3.2259 \\ -43.3013 \\ 0 \\ 0 \end{bmatrix} \tag{4.14}$$

- Proximal link:

$$\mathbf{w}_{dp_1} = \begin{bmatrix} 0 \\ 0 \\ 3.3125 \\ 43.3013 \\ 0 \\ 0 \end{bmatrix} \qquad \mathbf{w}_{bd_1} = \begin{bmatrix} 0 \\ 0 \\ -0.2165 \\ -43.3013 \\ 0 \\ 0 \end{bmatrix} \tag{4.15}$$

where forces are in N and moments in Nm.

# Chapter 5

# Finite Element Static Analysis

In order to understate a stress analysis the structure, we performed a static finite element analysis (FEA) with the Pro/Mechanica Structure module of Pro/Engineer, since all the previous work on the *Agile Wrist* was done with this software package. The finite element analysis enables us to calculate not only stresses but also deformation and strains, and thus, to verify whether the links can withstand the loads and where they are likely to break.

## 5.1 Material

To improve the stiffness of the links we focus on the geometry rather than on material selection, the optimization procedure being made assuming aluminium AL2014, which is used for general mechanical equipment, aeronautics and ordinance. Its characteristics are listed below (Memotech 1992, Pechiney data):

| | |
|---|---|
| Description: | Aluminium, wrought, 2014-T6 |
| Properties: | Structural isotropy |
| Mass density: | 2793.54 kg/m$^3$ |
| Young Modulus: | $7.30844 \times 10^{10}$ Pa |
| Poisson ratio: | 0.33 |
| Coefficient of thermal expansion: | $2.304 \times 10^{-5}$ |
| Allowed tensile stress: | $480 \times 10^{+6}$ Pa |
| Conventional elasticity limit at 0.2%: | $420 \times 10^{+6}$ Pa |
| Allowed sheared stress: | $290 \times 10^{+6}$ Pa |

## 5.2 Accuracy

The results given by the static analysis are approximated. The accuracy of the results depends on many parameters such as the way we define the loads and the constraints, the nature and the number of the finite elements, the polynomial degree of the approximation for the stress, strains and displacements. An idea about the accuracy of the results can be obtained by specifying a convergence tolerance. To perform the static analysis, we decided to use a multi-pass adaptive algorithm: the Pro/Mechanica Structure module performs the calculation for the static analysis by increasing the polynomial order of the approximation until the convergence